PERGAMON International Journal of Non-Linear Mechanics 37 (2002) 1319–1335

INTERNATIONAL JOURNAL OF
NON-LINEAR
MECHANICS

www.elsevier.com/locate/ijnonlinmec

Inversion of Ramberg–Osgood equation and description of hysteresis loops

Naser Mostaghel *, Ryan A. Byrd

Department of Civil Engineering, University of Toledo, Toledo, OH 43606, USA

Abstract

The Ramberg–Osgood equation has been approximately inverted. Four orders of approximations providing progressively more accurate inversions are considered. The second order inversion is used to develop closed-form relations for stress in terms of strain and for cyclic stress in terms of cyclic strain. Explicit relations between the cyclic-strength coefficient and the cyclic strain-hardening exponent and between the cyclic strain-hardening exponent and the elastic modulus are developed. Application to nine different engineering metals shows that the proposed approximate inversion provides a powerful tool for describing stress–strain relations. Examples of hysteresis loops for a number of strain time-histories are presented. Also, it is shown that augmenting the strain time-history with fictitious strain segments to close all the hysteresis loops yields the same stress–strain relation as that obtained through the rain-flow counting method.

Keywords: Ramberg–Osgood; Hysteresis; Non-linear; Elastic; Plastic; Stress; Strain

1. Introduction

The Ramberg–Osgood relation is commonly used to represent the cyclic as well as monotonic stress–strain curves. It provides a smooth continuous curve, with no distinct yield point, describing the total strain in terms of stress. It can be used to represent the behavior of many materials and systems. It has been used in conjunction with Neuber's rule to estimate the local notch stress and strain and the residual stress and strain after removal of the load. It has also been used to characterize hysteresis loop curves and fatigue life for various metals, alloys, and polymers. Fatemi and Yang [1] give a summary of various cumulative fatigue damage and life prediction theories. Saab and Nethercot [2], using a Ramberg–Osgood relation, modeled steel frame behavior under fire conditions. Mazzolani and Piluso [3], by using the Ramberg–Osgood relation to represent the moment curvature, formulated a procedure to predict the rotational capacity of aluminum alloy beams. Kaleta and Zietek [4] have shown a modified Ramberg–Osgood model to be a good approximation to the actual cyclic behavior of alpha-brass. Wong and Mai [5], based on the Ramberg–Osgood framework, investigated the effects of a rubber compound on the mechanical and fracture properties of an impact-modified nylon. Hight and Brandeau [6], using the Ramberg–Osgood relation, developed a mathematical model of the stress–strain and strain rate behavior of bone. Skelton et al. [7], by comparing the Ramberg–Osgood interpretation of

* Corresponding author. Tel.: +1-419-5308131; fax: +1-419-5308116.
E-mail address: nmostag@utnet.utoledo.edu (N. Mostaghel).

0020-7462/02/$ - see front matter
PII: S0020-7462(02)00025-2

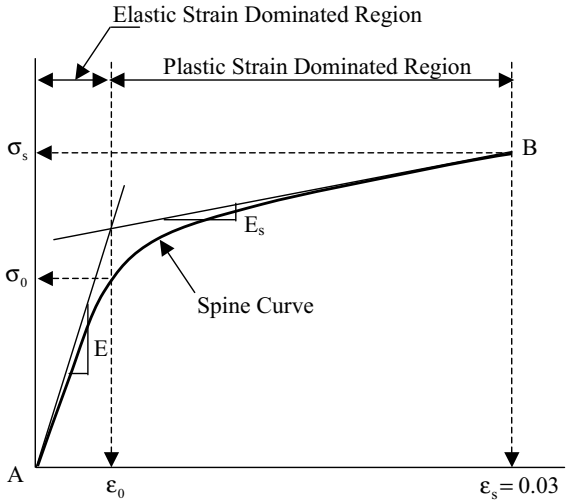

Fig. 1. Typical stress–strain curve.

stress–strain response and the relationships among the various Masing-type models, developed relationships to evaluate the expended and stored energies during monotonic as well as cyclic loading. In all these applications, because of the lack of a closed-form inversion of the Ramberg–Osgood relation for the description of stress in terms of strain, one has to employ either graphical or numerical techniques to evaluate the quantities of interest. Also in many practical situations stress is needed in terms of strain. This is because strain can be directly measured by a variety of experimental techniques, but stress can only be evaluated through analysis. Finite element analysis is often used to approximately evaluate the stresses. Here also basically the strains are evaluated first and then the stresses are calculated based on the strains. The inversion of the Ramberg–Osgood relation, which provides a description of stress in terms of strain, will be very useful to improve computation efficiency and reduce the lack of convergence problems. It also considerably simplifies the evaluation of the stress–strain relation and the construction of the hysteresis loops.

An analytical description of smooth hysteresis loops was initially formulated by Bouc [8] and later generalized by Wen [9,10]. Baber and Noori [11], Noori et al. [12], and Foliente et al. [13] extended the Wen model to include degradation and pinching effects. Ahmadi et al. [14] introduced a new term in the Wen model to make it thermodynamically consistent. Mostaghel [15] developed an analytical description of the hysteresis loops for deteriorating systems and used it to evaluate the response of a three degree of freedom system to harmonic and impulsive loads [16]. Sivaselvan and Reinhorn [17] pointed out the unifying concepts underlying a number of models for the construction of the hysteresis loops. Mayergoyz [18] gives comprehensive mathematical models of hysteresis.

The purpose of the work presented here is to approximately invert the Ramberg–Osgood relation and develop a closed-form description of stress in terms of strain, then, using this description, to develop closed-form expressions to describe both stress and cyclic stress as functions of time for any given strain time-history. Then the strain time-history and its corresponding cyclic stress time-history can be used to construct the hysteresis loops.

To this end, as shown in Fig. 1, the stress–strain space is divided into elastic strain dominated and plastic strain dominated regions. In the elastic strain dominant region, a power law is used to describe the stress in terms of the total strain. In the plastic strain dominant region, the Ramberg–Osgood relation, which is also a power law, is expanded in a binomial series, and the first five terms of the series are used to construct

a polynomial involving elastic strain up to the fourth power. By considering progressively higher powers in this polynomial and by matching the continuity of both stress and its slope at the interface of the two regions, four orders of approximate inversions are developed. Detailed descriptions of the first two orders are presented here. To show the quality of the proposed inversions, the cyclic stress–strain curves for nine different metals are prepared and superimposed on their corresponding Ramberg–Osgood curves. The maximum percentage difference for each case and for each order of approximation is evaluated. Considering the fact that these differences are small, and considering the fact that the Ramberg–Osgood relation is an approximate representation, it is proposed to use the expression for the second order inversion as a standard representation of stress in terms of strain. Based on the second order inversion, equations for explicit evaluation of cyclic stress, for the description of hysteresis loops, are developed. Examples of application to various cyclic strain histories are presented which show the promise of the proposed representation in simplifying the solution process. In particular, through an example, it is shown that augmenting the strain time-history with fictitious strain segments to close all the hysteresis loops, as the stress–strain relation evolves, yields the same stress–strain relation as that obtained through the rain-flow counting method. Also, an explicit relation between the Ramberg–Osgood parameters is developed and used in the proposed formulation. It should be noted that the proposed inversion expression could also be used to describe the monotonic stress–strain relations for materials which do not exhibit a distinct yield point. For the monotonic stress–strain relations, the cyclic parameters must be replaced by their corresponding monotonic parameters.

2. Formulation

The Ramberg–Osgood stress–strain relation is defined by

$$\varepsilon = \frac{\sigma}{E} + \left(\frac{\sigma}{K'}\right)^{1/n'}, \tag{1}$$

where σ is the stress, ε is sum of the elastic strain

$$\varepsilon_e = \frac{\sigma}{E} \tag{2}$$

and the plastic strain

$$\varepsilon_p = \left(\frac{\sigma}{K'}\right)^{1/n'}, \tag{3}$$

E is the modulus of elasticity, K' is the cyclic-strength coefficient, and n' is the cyclic strain-hardening exponent. It should be noted that, for cyclic applications, the strain, ε, and the stress, σ, in the above relations are the cyclic amplitude of these quantities. To express σ in terms of the total strain, ε, consider Fig. 1. This figure represents a plot of Eq. (1). ε_s is an assumed supreme strain, and σ_s is its corresponding supreme stress. The plot is divided into two regions, one dominated by elastic strain and the other by plastic strain. In the elastic strain dominated region, it is assumed that the following power law can represent σ as a function of the total strain ε:

$$\sigma = E\varepsilon - \alpha\varepsilon^{\beta}. \tag{4}$$

The parameters α and β are evaluated by matching the stress and its slope at the interface of the elastic dominated and the plastic dominated regions. Denoting the interface strain by ε_0 and the value of the corresponding interface stress and its slope by σ_0 and E_0, respectively, it can be shown that

$$\alpha = \frac{E\varepsilon_0 - \sigma_0}{\varepsilon_0^{\beta}}, \tag{5}$$

$$\beta = \frac{(E - E_0)\varepsilon_0}{E\varepsilon_0 - \sigma_0}. \tag{6}$$

To develop the stress–strain relation for the plastic dominated region, first the Ramberg–Osgood equation is expressed in terms of strains, i.e.,

$$\frac{E}{K'}\,\varepsilon_e = \left(1 - \frac{\varepsilon_e}{\varepsilon}\right)^{n'} \varepsilon^{n'}. \tag{7}$$

Expanding the right-hand side of the above relation in a binomial series and including terms up to the fourth order yields

$$\varepsilon_e = \frac{K'}{E}\,\varepsilon^{n'}\left[1 - n'\left(\frac{\varepsilon_e}{\varepsilon}\right) + \frac{n'(n'-1)}{2}\left(\frac{\varepsilon_e}{\varepsilon}\right)^2 - \frac{n'(n'-1)(n'-2)}{6}\left(\frac{\varepsilon_e}{\varepsilon}\right)^3 + \frac{n'(n'-1)(n'-2)(n'-3)}{24}\left(\frac{\varepsilon_e}{\varepsilon}\right)^4\right]. \tag{8}$$

Rearranging the terms, this equation can be written as

$$a + b\varepsilon_e + c\varepsilon_e^2 + d\varepsilon_e^3 + e\varepsilon_e^4 = 0, \tag{9}$$

where

$$a = \varepsilon^{n'}, \tag{10}$$

$$b = -\left(\frac{E}{K'} + n'\varepsilon^{n'-1}\right), \tag{11}$$

$$c = \frac{n'(n'-1)\varepsilon^{n'-2}}{2}, \tag{12}$$

$$d = -\frac{n'(n'-1)(n'-2)\varepsilon^{n'-3}}{6}, \tag{13}$$

$$e = \frac{n'(n'-1)(n'-2)(n'-3)\varepsilon^{n'-4}}{24}. \tag{14}$$

Four orders of approximation are possible. In the following the first and the second approximations are presented in detail. Relations yielding the third and the fourth approximations are given in Appendix A.

2.1. First order approximation

The first order approximation is to consider only the terms with power $\leqslant 1$ in Eq. (9). This would reduce this equation to

$$a + b\varepsilon_e = 0. \tag{15}$$

Substituting for a and b into the above equation and considering relation (2), it can be shown that

$$\sigma_1 = \frac{K'\varepsilon^{n'}}{1 + (K'/E)n'\varepsilon^{n'-1}}. \tag{16}$$

The subscript 1 on σ denotes the first order approximation. To consider the effects of the higher order terms dropped from Eq. (15) on the stress at large values of the plastic strain, the following correction term will

be added to the above relation:

$$\delta\sigma_1 = \sigma_s - \frac{K'\varepsilon_s^{n'}}{1 + (K'/E)n'\varepsilon_s^{n'-1}}. \tag{17}$$

The above correction term is evaluated by matching the value of the stress at $\varepsilon = \varepsilon_s$. Therefore, the first order corrected stress in the plastic region is given by

$$\sigma_1 = \frac{K'\varepsilon^{n'}}{1 + (K'/E)n'\varepsilon^{n'-1}} + \delta\sigma_1. \tag{18}$$

Before Eqs. (4) and (18) can be used, one needs to define the value of the interface strain, ε_0. As shown on Fig. 1, ε_0 is the value of strain at the intersections of lines tangent to the Ramberg–Osgood curve at $\varepsilon = 0$ and ε_s. This strain is given by

$$\varepsilon_0 = \frac{\sigma_s - E_s\varepsilon_s}{E - E_s}, \tag{19}$$

where $\sigma_s = \sigma(\varepsilon_s)$, and from Eq. (1)

$$E_s = \frac{d\sigma(\varepsilon_s)}{d\varepsilon} = \frac{E}{1 + E/n'(K')^{-1/n'}(\sigma_s)^{1/n'-1}}. \tag{20}$$

Taking the logarithm of both sides of Eq. (1) and replacing σ by σ_s and ε by ε_s, it can be shown that

$$K' = \frac{\sigma_s}{(\varepsilon_s - \sigma_s/E)^{n'}}. \tag{21}$$

Using this relation one can show that

$$(K')^{-1/n'}(\sigma_s)^{1/n'-1} = \frac{\varepsilon_s - \sigma_s/E}{\sigma_s}. \tag{22}$$

Substituting from the above equation into Eq. (20) yields

$$E_s = \frac{\sigma_s}{\sigma_s/E + (1/n')(\varepsilon_s - \sigma_s/E)}. \tag{23}$$

Finally, to evaluate β from Eq. (6), one needs to evaluate E_0 first. Denoting the interface slopes for the first order approximation by E_{01} and using Eq. (18), it can be shown that

$$E_{01} = \frac{d\sigma_1(\varepsilon_0)}{d\varepsilon} = -\frac{n'(n'-1)K'^2\varepsilon_0^{2(n'-1)}}{E(1 + K'n'\varepsilon_0^{(n'-1)}/E)^2} + \frac{K'n'\varepsilon_0^{(n'-1)}}{1 + K'n'\varepsilon_0^{(n'-1)}/E}. \tag{24}$$

Now according to Eqs. (5) and (6)

$$\alpha_1 = \frac{E\varepsilon_0 - \sigma_{01}}{\varepsilon_0^{\beta}}, \tag{25}$$

$$\beta_1 = \frac{(E - E_{01})\varepsilon_0}{E\varepsilon_0 - \sigma_{01}}. \tag{26}$$

Again the subscript 1 on α and β denotes the fact that these parameters are for the first order approximation. Now using Eqs. (4) and (18) in conjunction with Eqs. (25) and (26), the first order approximation of the function defining the stress in terms of strain over the whole range of $\varepsilon = 0$ to ε_s is given by

$$\sigma_1 = N(E\varepsilon - \alpha_1\varepsilon^{\beta_1}) + M\left(\frac{K'\varepsilon^{n'}}{1 + (K'/E)n'\varepsilon^{n'-1}} + \delta\sigma_1\right), \tag{27}$$

where σ_1 represents the first order approximation and N and M are switching functions defined by Mostaghel [15] as

$$N = 0.5(1 + \mathrm{sgn}(\varepsilon_0 - \varepsilon))(1 + (1 - \mathrm{sgn}(\varepsilon_0 - \varepsilon))), \tag{28}$$

$$M = 0.5(1 - \mathrm{sgn}(\varepsilon_0 - \varepsilon))(1 - (1 + \mathrm{sgn}(\varepsilon_0 - \varepsilon))), \tag{29}$$

where sgn is the signum function.

To get an idea of the errors involved in the representation of the inversion of Eq. (1) by Eq. (27), let σ_0 denote the value of the stress at $\varepsilon = \varepsilon_0$ as calculated from the Ramberg–Osgood Eq. (1). Since σ_{01} represents the value of the stress from Eq. (27) for the interface strain, ε_0, then the percentage error for the first order inversion is given by

$$\eta_1 = \frac{\sigma_{01} - \sigma_{\mathrm{RO}}}{\sigma_{\mathrm{RO}}}(100), \tag{30}$$

where $\sigma_{\mathrm{RO}} = \sigma(\varepsilon_0)$ as evaluated from Eq. (1).

2.2. Second order approximation

For the second order approximation, Eq. (9) reduces to

$$a + b\varepsilon_{\mathrm{e}} + c\varepsilon_{\mathrm{e}}^2 = 0. \tag{31}$$

Substituting for a, b, and c from Eqs. (10) to (12) into Eq. (31) and solving the resulting polynomial, it can be shown that

$$\sigma_2 = E\left[\frac{E}{K'} + n'\varepsilon^{n'-1} - \sqrt{\left(\left(\frac{E}{K'} + n'\varepsilon^{n'-1}\right)^2 - 2n'(n'-1)\varepsilon^{2(n'-1)}\right)}\right] \Big/ (n'(n'-1)\varepsilon^{n'-2}) + \delta\sigma_2, \tag{32}$$

where the correction term $\delta\sigma_2$ is given by

$$\delta\sigma_2 = \sigma_{\mathrm{s}} - E\left[\frac{E}{K'} + n'\varepsilon_{\mathrm{s}}^{n'-1} - \sqrt{\left(\left(\frac{E}{K'} + n'\varepsilon_{\mathrm{s}}^{n'-1}\right)^2 - 2n'(n'-1)\varepsilon_{\mathrm{s}}^{2(n'-1)}\right)}\right] \Big/ (n'(n'-1)\varepsilon_{\mathrm{s}}^{n'-2}). \tag{33}$$

Denoting the interface slope at $\varepsilon = \varepsilon_0$ for the second order approximation by E_{02} and using Eq. (32), it can be shown that

$$E_{02} = \frac{\mathrm{d}\sigma_2(\varepsilon_0)}{\mathrm{d}\varepsilon} = \frac{E}{n'(n'-1)}\left\{(2-n')\varepsilon_0^{-1+n'}\left[\left(\frac{E}{K'} + n'\varepsilon_0^{-1+n'}\right) - \sqrt{\begin{matrix}-2n'(n'-1)\varepsilon_0^{-2+2n'} \\ +\left(\frac{E}{K'} + n'\varepsilon_0^{-1+n'}\right)^2\end{matrix}}\right]\right\}$$

$$+E\left(1 - \frac{2\left(\frac{E}{K'} + (n' - 2(n'-1))\varepsilon_0^{-1+n'}\right)}{2\sqrt{-2n'(n'-1)\varepsilon_0^{-2+2n'} + \left(\frac{E}{K'} + n'\varepsilon_0^{-1+n'}\right)^2}}\right). \tag{34}$$

The parameters α and β in Eqs. (5) and (6) for the second order approximation are given by

$$\alpha_2 = \frac{E\varepsilon_0 - \sigma_{02}}{\varepsilon_0^{\beta_2}}, \tag{35}$$

$$\beta_2 = \frac{(E - E_{02})\varepsilon_0}{E\varepsilon_0 - \sigma_{02}}. \tag{36}$$

Therefore, using definitions (28) and (29), the second order approximation of the function defining the stress in terms of strain over the whole range of $\varepsilon = 0$ to ε_s can be represented by

$$\sigma_2 = N(E\varepsilon - \alpha_2\varepsilon^{\beta_2}) + M\left\{E\left[\frac{E}{K'} + n'\varepsilon^{n'-1} - \sqrt{\left(\left(\frac{E}{K'} + n'\varepsilon^{n'-1}\right)^2 - 2n'(n'-1)\varepsilon^{2(n'-1)}\right)}\right]\Big/ (n'(n'-1)\varepsilon^{(n'-2)}) + \delta\sigma_2\right\}. \tag{37}$$

Also the error associated with the second order inversion is given by

$$\eta_2 = \frac{\sigma_{02} - \sigma_0}{\sigma_0}(100). \tag{38}$$

It should be noted that for a given ε_s, σ_s if E and E_s can be evaluated from the given data, then Eq. (23) implies that

$$n' = \left(\frac{\varepsilon_s - \sigma_s/E}{1 - E_s/E}\right)\left(\frac{E_s}{\sigma_s}\right). \tag{39}$$

3. Comparisons

To show the quality of the proposed approximate inversions, first, as examples, based on Eq. (1) the stress–strain curves for nine different engineering metals for cyclic strains up to $\varepsilon_s = 0.03$ are plotted in Figs. 2–10. Then for comparison purposes, using Eqs. (27) and (37), the stress–strain curves for each metal, for the first and the second approximations, are superimposed on the corresponding figures, respectively. Using the terms involving the third and the fourth powers in Eq. (9), the basic relations needed to define the third and the fourth approximations are developed and presented in Appendix A. Because the equations are very

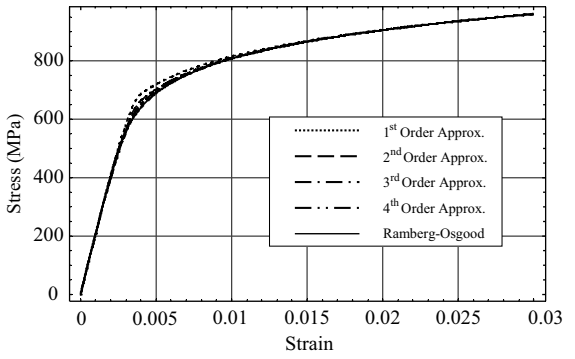

Fig. 2. Cyclic stress–strain curve for 8630-cast steel.

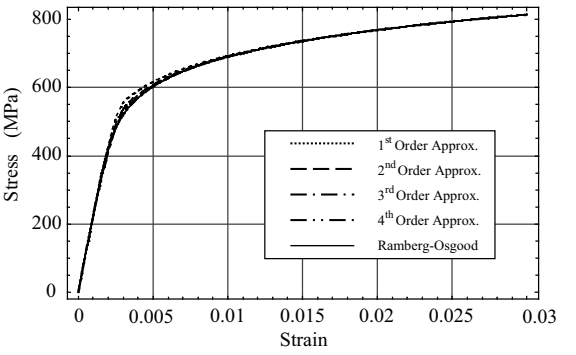

Fig. 3. Cyclic stress–strain curve for 1141-Q& T steel.

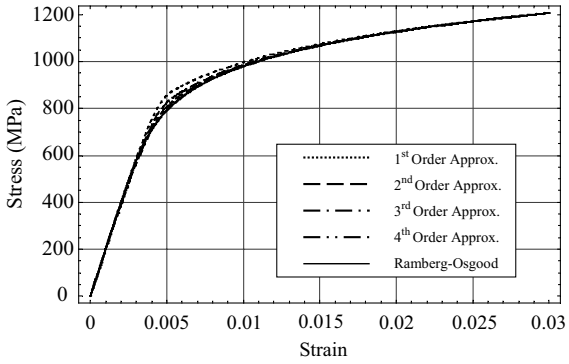

Fig. 4. Cyclic stress–strain curve for 4340-Q& T steel.

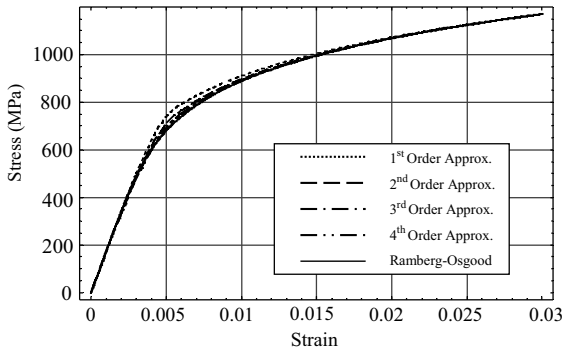

Fig. 5. Cyclic stress–strain curve for 304-CD steel.

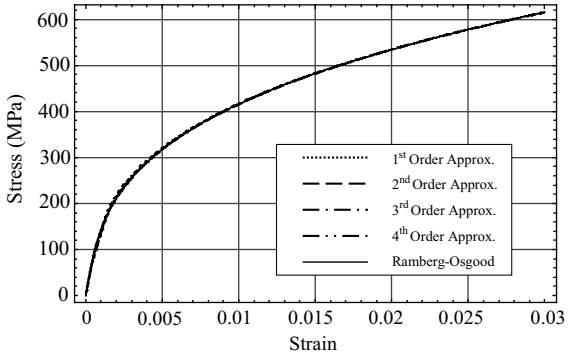

Fig. 6. Cyclic stress–strain curve for 1020-HR sheet steel.

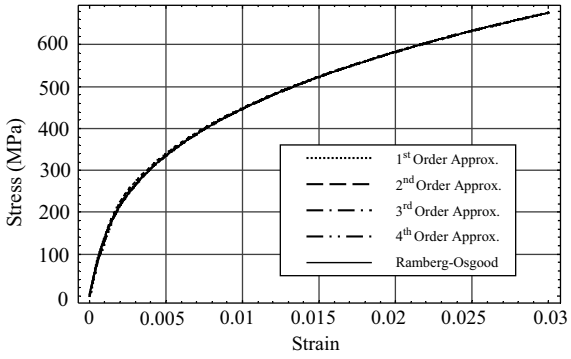

Fig. 7. Cyclic stress–strain curve for 304-annealed steel.

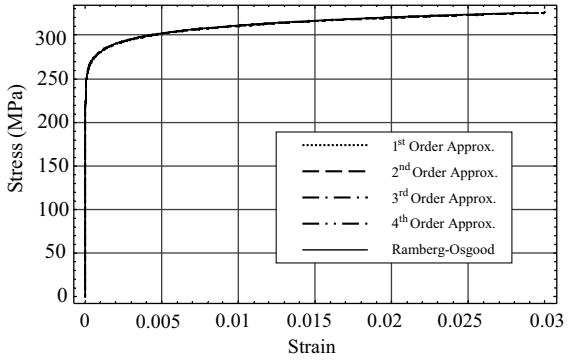

Fig. 8. Cyclic stress–strain curve for A356-cast aluminum.

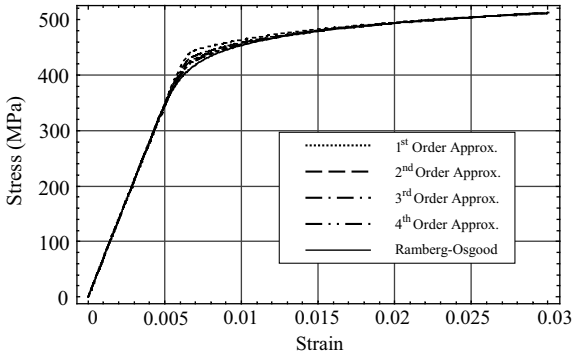

Fig. 9. Cyclic stress–strain curve for 2024-T3 aluminum.

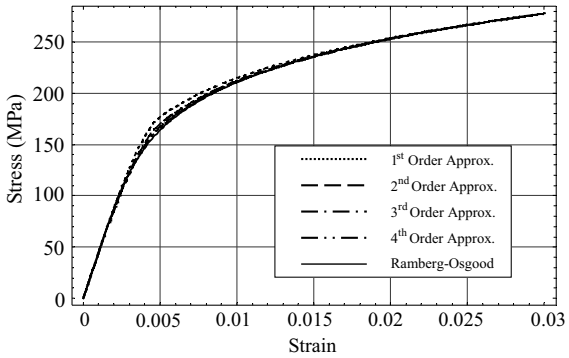

Fig. 10. Cyclic stress–strain curve for AZ91E-T6 cast magnesium.

Table 1
Comparisons of maximum errors associated with the four approximate inversions

Material[a]	E	n'	K'	σ_0	σ_y[b]	% maximum error			
	(GPa)		(MPa)	(MPa)	(MPa)	η_1	η_2	η_3	η_4
8630-cast steel	207	0.122	1502	643.5	703.7	6.5	3.2	1.8	1.1
1141-Q& T steel	227	0.124	1277	528.6	590.9	6.5	3.2	1.8	1.1
4340-Q& T steel	200	0.135	1996	804.5	862.6	7.9	4.1	2.4	1.5
304-CD steel	172	0.176	2270	717.3	760.3	8.2	4.1	2.2	1.3
1020-HR sheet steel	203	0.321	1962	213.9	266.9	4.0	1.2	0.4	0.2
304-annealed steel	190	0.334	2275	235.8	285.4	4.2	1.3	0.5	0.2
A356-cast aluminum	70	0.034	379	232.0	290.1	2.7	1.5	0.9	0.6
2024-T3 aluminum	70	0.065	655	415.4	437.3	6.9	4.4	3.0	2.2
AZ91E-T6 cast Mg	45	0.184	552	164.3	175.9	7.9	3.8	2.0	1.1

[a] E, n', and K' are from [19].
[b] σ_y is based on 0.2% offset strain.

lengthy, they are not presented here. However, to see the quality of the improvement generated by these approximations, for the given examples, the third and the fourth approximate stress–strain curves are also included in Figs. 2–10. The error associated with each approximation is also evaluated and reported in Table 1. The proposed approximate inversions are applicable for monotonic as well as cyclic stress–strain curves. Here Figs. 2–10 are based on the cyclic Ramberg–Osgood parameters as given by Stephens et al. [19]. These parameters are also presented in Table 1. To keep track of the lengthy expressions involved in the third and the fourth approximations, a computer code in Wolfram's Mathematica [20] has been developed.

Considering Figs. 2–10, it is clear that the proposed approximations progressively provide higher quality inversions of the Ramberg–Osgood equation. Also it is apparent that the calculated errors are based on the maximum deviation from the Ramberg–Osgood equation. As seen from Table 1, these errors are relatively small, and their values reduce as higher order approximations are utilized.

As a specific example of comparison, consider a material with an initial modulus $E = 69,000$ MPa, and a uniaxial stress–strain curve characterized by the cyclic-strength coefficient $K' = 690$ MPa, and the cyclic strain-hardening exponent $n' = 0.15$. We would like to estimate the stress–strain response starting from zero and then cycling between $\varepsilon_{\max} = 0.028$ and $\varepsilon_{\min} = 0.01$. We need to evaluate the stress coordinates $\sigma_{\max}$ and $\sigma_{\min}$ associated with the given strain coordinates $\varepsilon_{\max}$ and $\varepsilon_{\min}$.

Table 2
Comparisons of solutions for the example application

Solutions	σ_{max} (MPa)	σ_{min} (MPa)	% error	$\delta\sigma$ (MPa)
First approx.	391.31	− 237.76	5.9	− 1.16
Second approx.	390.29	− 228.81	1.9	− 0.14
Third approx.	390.17	− 226.01	0.7	− 0.02
Fourth approx.	390.15	− 225.02	0.3	0.00
Dowling[a]	390.15	− 224.40	0.0	0.00

[a]Example 12.4, [21].

For the unloading branch, the material behaves in a manner consistent with the kinematic hardening rule. Considering this rule and Eq. (1), it can be shown that

$$\Delta\varepsilon = \varepsilon_{max} - \varepsilon_{min} = \frac{\Delta\sigma}{E} + 2\left(\frac{\Delta\sigma}{2K'}\right)^{1/n'} = \frac{\Delta\sigma}{E} + \left(\frac{\Delta\sigma}{K'_e}\right)^{1/n'}, \tag{40}$$

where

$$K'_e = 2^{(1-n')}K', \tag{41}$$

$$\Delta\sigma = \sigma_{max} - \sigma_{min}. \tag{42}$$

Choosing to invert Eq. (40) according to the second order approximation defined by Eq. (37) yields

$$\Delta\sigma_2 = N(E\varepsilon - \alpha_2\varepsilon^{\beta_2}) + M\left\{E\left[\frac{\frac{E}{K'_e} + n'(\Delta\varepsilon)^{n'-1}}{n'(n'-1)(\Delta\varepsilon)^{(n'-2)}} - \frac{\sqrt{\left(\left(\frac{E}{K'_e} + n'(\Delta\varepsilon)^{n'-1}\right)^2 - 2n'(n'-1)(\Delta\varepsilon)^{2(n'-1)}\right)}}{n'(n'-1)(\Delta\varepsilon)^{(n'-2)}}\right]\right\}. \tag{43}$$

It should be noted that for the first term in the above relation, ε has not been replaced by $\Delta\varepsilon$ because for this term to have a non-zero value ε must be $\leqslant \varepsilon_0$, i.e., for this term the behavior is within the elastic strain dominated region and as such it is assumed that the behavior is elastic. This does not impose any restriction for applications involving very small strains. In these cases the value of ε_0 can be reduced to the range of interest by choosing a smaller ε_s and its corresponding σ_s and E_s for substitution into Eq. (19) to evaluate ε_0.

For our example $\Delta\varepsilon = \varepsilon_{max} - \varepsilon_{min} = 0.028 - 0.01 = 0.018$. Substitution of this value for $\Delta\varepsilon$ into the above equation yields $\Delta\sigma_2 = 619.10$ Mpa. Letting $\varepsilon = \varepsilon_{max} = 0.028$ into Eq. (37) yields $\sigma_{max\,2} = 390.29$ MPa. Therefore, according to Eq. (42)

$$\sigma_{min\,2} = \sigma_{max\,2} - \Delta\sigma_2 = 390.29 - 619.10$$
$$= -228.81 \text{ MPa}. \tag{44}$$

Dowling [21], using the Ramberg–Osgood Eq. (1), has solved this very example and has obtained a $\sigma_{min} = -224.4$ MPa. Therefore, the error associated with the second order approximation for this example is

$$\mu_2 = 100(\sigma_{min} - \sigma_{min\,2})/\sigma_{min} = 1.9\%. \tag{45}$$

Similar calculations have been carried out for other approximations, and the results together with the associated errors are presented in Table 2. The error for the third order approximation is 0.7%, which reduces to 0.3% for the fourth order approximation. It should be noted that in this example the matching correction term $\delta\sigma_2$

is small and is neglected. If one wants to include the $\delta\sigma$ term, then one should evaluate $\sigma_{\max}$ directly from the Ramberg–Osgood equation rather than from the proposed approximate equations. Using the Ramberg–Osgood equation, one finds $\sigma_{\max} = 390.15$ MPa, which is very close to the value $\sigma_{\max 2} = 390.29$ MPa found from Eq. (37). The matching correction terms, $\delta\sigma$, for all orders of approximations are presented in Table 1. It should be noted that in this example $\varepsilon_{\max} > \varepsilon_0$. As such the first term of Eq. (43) is identically zero.

4. Cyclic applications

To show the capability of Eqs. (37) and (43) in presenting cyclic stress–strain relations, as an example, consider a material with a cyclic-strength coefficient $K' = 1502$ MPa, and a cyclic strain-hardening exponent $n' = 0.122$. If a sample of this material is subjected to the multiple step strain histories shown in Figs. 11a, 12a, and, 13a, the corresponding stress–strain relations will be as shown in Figs. 11b, 12b, and 13b. The following procedure is used to develop these figures. First, for each case, the strain time-history is represented by

$$\varepsilon = \sum_{i=1}^{k} \phi_i(a_{i-1} + b_i(t - t_{i-1})), \tag{46}$$

where a_i is the strain amplitude at time t_i and b_i is given by

$$b_i = \frac{a_{i+1} - a_i}{t_{i+1} - t_i}. \tag{47}$$

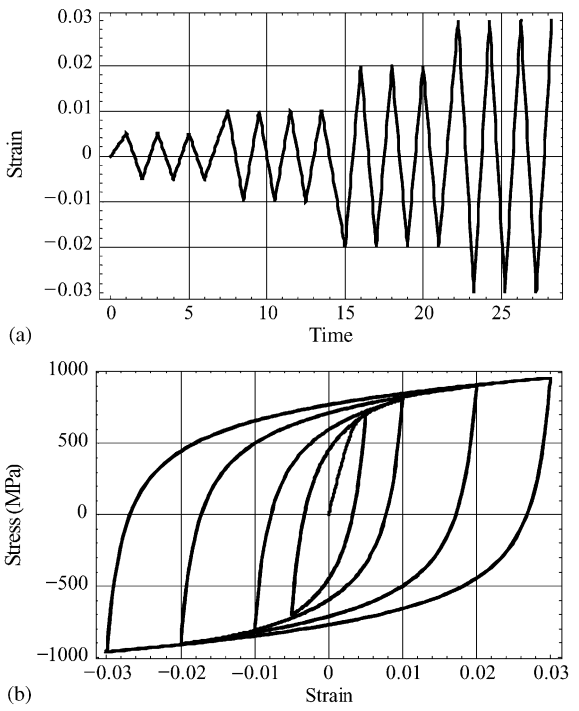

Fig. 11. (a) A multi-step strain time-history; (b) stress–strain relation.

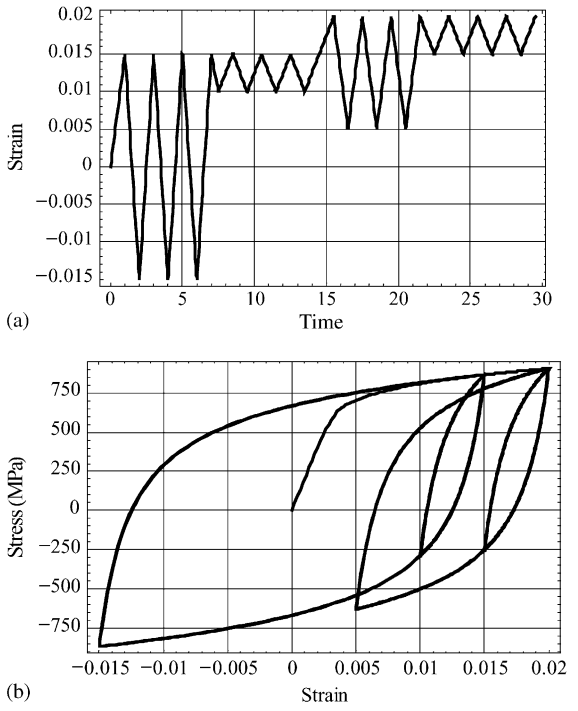

Fig. 12. (a) A multi-step strain time-history; (b) stress–strain relation.

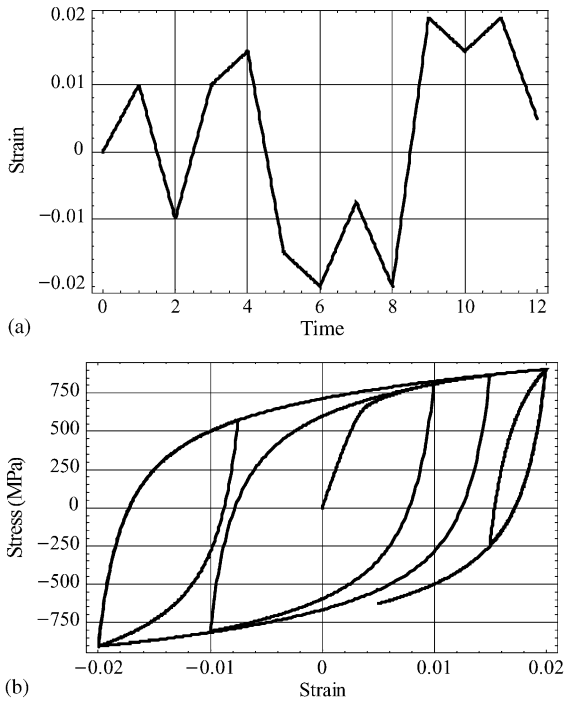

Fig. 13. (a) A multi-step strain time-history; (b) stress–strain relation.

The time-tracking function ϕ_i, whose value is either 0 or 1, is defined by

$$\phi_i = N_i - N_{i-1}, \tag{48}$$

where the switching functions N_i are given by

$$N_i = 0.5((1 + \mathrm{sgn}(t_i - t))(1 + (1 - \mathrm{sgn}(t_i - t))) \tag{49}$$

and sgn is the signum function. Second, the strain amplitude as a function of time is represented by

$$a = \sum_{i=1}^{k} \phi_i a_{i-1}. \tag{50}$$

Now the strain change as a function of time is represented by

$$\Delta\varepsilon = |a - \varepsilon| \tag{51}$$

and the change in strain amplitudes as a function of time is represented by

$$(\Delta\varepsilon)_i = |a_{i+1} - a_i|. \tag{52}$$

Substitution for $\Delta\varepsilon$ from Eq. (51) into Eq. (43) yields the absolute value of $\Delta\sigma_2$. Since it is understood that the whole development is based on the second order approximation, the subscript 2 is dropped. Therefore, the cyclic stress change, $\Delta\sigma$, as a function of time is given by

$$\Delta\sigma = |\Delta\sigma|\,\mathrm{sgn}(\dot{\varepsilon}), \tag{53}$$

where dot denotes differentiation with respect to time, and the strain rate, $\dot{\varepsilon}$, as obtained from Eq. (46), is given by

$$\dot{\varepsilon} = \sum_{i=1}^{k} \phi_i b_i. \tag{54}$$

Substitution for $(\Delta\varepsilon)_i$ from Eq. (52) into Eq. (43) yields the change in stress amplitude between successive strain amplitudes as $(\Delta\sigma)_i$. Then the cyclic stress amplitudes, σ_{i+1}, are given by

$$\sigma_{i+1} = \sigma_i + (\Delta\sigma)_i \operatorname{sgn}(b_{i+1}). \tag{55}$$

Now the cyclic stress amplitude as a function of time can be represented by

$$\sigma_a = \sum_{i=1}^{k} \phi_i \sigma_{i-1}. \tag{56}$$

The value of σ_1 in relation (55) is the stress amplitude as given by Eq. (37) for the strain amplitude a_1 and $\sigma_0 = 0$ in the above equation. Third, combining Eqs. (53) and (56) yields the cyclic stress as a function of time (from *time zero* to time t) as

$$\sigma = \phi_1 \tilde{\sigma} + (\sigma_a + \Delta\sigma), \tag{57}$$

where $\tilde{\sigma}$ is given by Eq. (37) and represents the spine curve which, besides being the locus of the strain and stress amplitudes on the stress–strain curve, is also the stress–strain relation during the time that strain varies from zero to strain amplitude a_1.

Eq. (57) yields correct stress–strain relations for single step tests. In these tests the magnitudes of the successive strain amplitudes are the same. An adjustment has to be introduced into Eq. (57) to make it applicable for more complex strain histories, particularly for the cases in which the strain amplitude increases/decreases from a positive/negative value to a higher/lower positive/negative value. The adjustment is necessary because in these cases the evolution of the stress–strain loops has to proceed on the spine curve. This adjustment changes Eq. (55) to

$$\sigma_{i+1} = \sigma_i + (\Delta\sigma)_i(1 - v_{i+1}) \operatorname{sgn}(b_{i+1}) + (\tilde{\sigma}_{i+1} - \tilde{\sigma}_i)(v_{i+1}) \operatorname{sgn}(b_{i+1}), \tag{58}$$

where the quantity v_i, whose value is either 1 or 0, is defined by

$$v_i = \frac{1 + \operatorname{sgn}(b_i) \operatorname{sgn}(b_{i-1})}{2}. \tag{59}$$

In the above equations $\tilde{\sigma}_i$ denotes the value of the stress obtained from Eq. (37) corresponding to the strain amplitude a_i, and b_i is defined by Eq. (47). Now substituting for σ_i from Eq. (58) into Eq. (56) and combining the results with Eq. (53) changes Eq. (57) to

$$\sigma = v\tilde{\sigma} + (\sigma_a + \Delta\sigma)(1 - v), \tag{60}$$

where

$$v = \sum_{i=1}^{k} \phi_i v_i \tag{61}$$

and $\tilde{\sigma}$ is given by Eq. (37). Eq. (60) represents cyclic stress as a function of time. Using Eq. (60) and (46), the stress–strain relations for the strain time-histories given in Figs. 11a to 13a are evaluated and presented in Figs. 11b to 13b, respectively. Eq. (60) directly yields the correct cyclic stress values as long as the strain time-history is such that at least one extreme point of any stress–strain loop touches the spine curve (extreme touching condition). This is true of all the loops shown in Figs. 11b to 13b. However, consider Figs. 14a and 14b. Here strain time-history is such that the stress–strain loops do not satisfy the extreme touching condition.

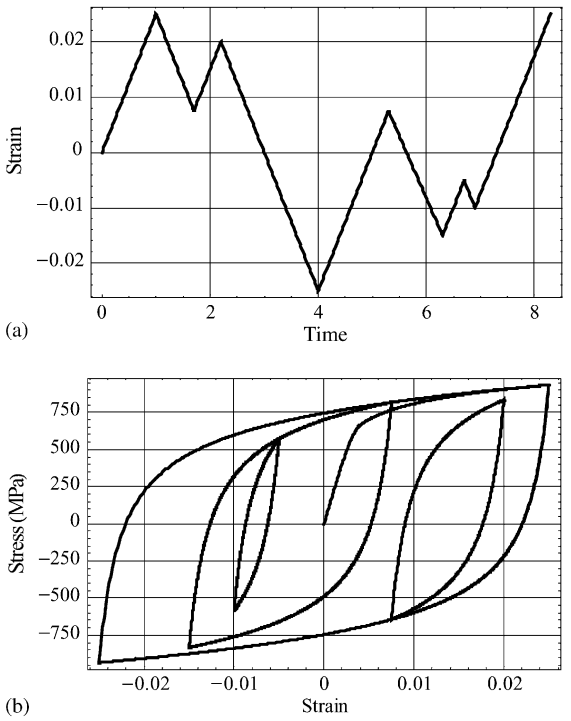

Fig. 14. (a) A multi-step irregular strain time-history; (b) stress–strain relation.

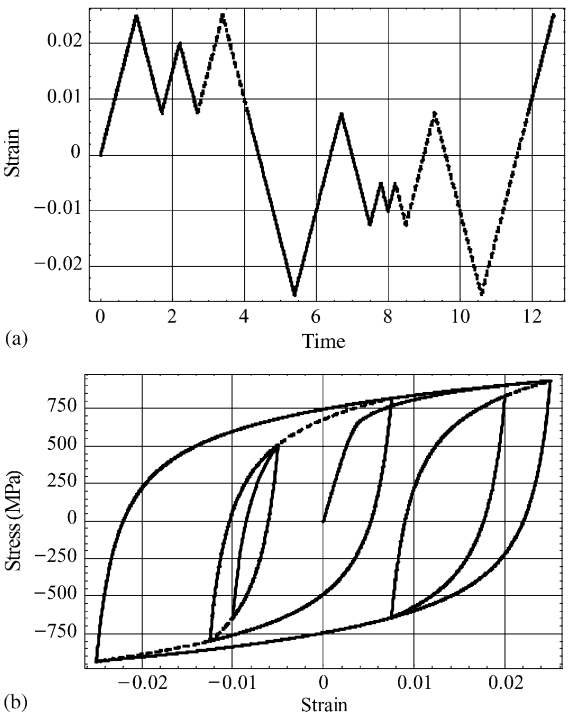

Fig. 15. (a) The augmented strain time-history; (b) stress–strain relation.

In this case Eq. (60) in conjunction with the rain-flow method presented by Ellyin [22] is used to develop the correct stress–strain relation shown in Fig. 14b. For cases of this type, using Eq. (60) yields approximate stress–strain relations. However, one can obtain the correct stress–strain relation using Eq. (60) without the use of the rain-flow method if one augments the strain time-history with fictitious strain segments to close all the hysteresis loops as the stress–strain relation evolves. As an example, the strain time-history of Fig. 14a is augmented with fictitious strain segments, shown in dashed lines in Fig. 15a. The corresponding stress–strain relation is shown in Fig. 15b, where the dashed curves correspond to parts of the fictitious strain segments shown in Fig. 15a. Except for the dashed curves, Fig. 15b is identical to Fig. 14b. Once the augmented strain time-history is defined, it is far easier to construct the hysteresis loops through Eq. (60) than through the rain-flow counting method.

5. Conclusions

The Ramberg–Osgood equation has been inverted approximately. Explicit analytical relations for the stress in terms of strain have been developed up to the fourth order. Even though it is possible to extend the process to higher order approximations numerically, with the procedure presented here it is impossible to develop any higher order explicit analytical relation for stress in terms of strain. This is due to the fact that there is no analytical rule to describe the roots for polynomials with power higher than four. For all the examples considered, the interface strain, ε_0 as defined in Fig. 1, is smaller than the yield strain based on 0.2% offset.

Therefore, the yield stress associated with 0.2% strain offset, as presented in Table 1, is significantly larger than the interface stress σ_0.

Eq. (21) provides an explicit relation between the Ramberg–Osgood parameters K' and n', and Eq. (39) presents the cyclic strain-hardening exponent, n', in terms of an expression involving the modulus of elasticity, the supreme stress and strain and the slope of the stress–strain curve, E_s, at the supreme strain, ε_s. In practice, it may be difficult to make an accurate estimate of E_s directly from the experimental data. One can avoid evaluating E_s by estimating n' as the slope of the line fitted to data of the log–log plot of stress versus plastic strain as described by Dowling. Once n' is known, then K' can be evaluated from Eq. (21). Figs. 2–10, involving a whole range of parameters n' and K', clearly establish the viability of the proposed approximate inversions. As seen in Table 2 the values of the stress corrections $\delta\sigma_i$'s for all levels of approximations are relatively small and negligible, particularly for the second and the higher order approximations. As such, Eq. (37) may be simplified by dropping the term $\delta\sigma_2$. Considering the values of $\delta\sigma_i$ presented in Table 2, and the magnitudes of errors presented in Tables 1 and 2, and considering the fact that the Ramberg–Osgood equation itself is an approximate fit to data, it is proposed to use Eq. (37), with $\delta\sigma_2$ set equal to zero, as the standard inversion relation.

Figs. 11b to 13b clearly show the power of Eq. (60) in mapping a cyclic strain time-history to a cyclic stress time-history that can be used to plot the stress–strain relation. Comparing Figs. 14a and 14b to their corresponding figures, 15a and 15b, it is clear that augmenting the strain time-history with fictitious strain segments yields hysteresis loops which are the same as those obtained through the rain-flow counting method.

Acknowledgements

The authors express their thanks to Dr. A. Fatemi, Professor of Mechanical Engineering at the University of Toledo, for many helpful discussions.

Appendix A. Third and fourth order solutions

For the third order approximation, Eq. (9) reduces to

$$a + b\varepsilon_e + c\varepsilon_e^2 + d\varepsilon_e^3 = 0. \tag{A.1}$$

The solution to this equation is given by

$$\varepsilon_e = E\left[\frac{\sqrt[3]{-2c^3 + 9bdc - 27ad^2 + \sqrt{4(3bd - c^2)^3 + (-2c^3 + 9bdc - 27ad^2)^2}}}{3\sqrt[3]{2}d} - \frac{c}{3d}\right.$$

$$\left. - \frac{\sqrt[3]{2}(3bd - c^2)}{3d\sqrt[3]{-2c^3 + 9bdc - 27ad^2 + \sqrt{4(3bd - c^2)^3 + (-2c^3 + 9bdc - 27ad^2)^2}}}\right], \tag{A.2}$$

where a, b, c, and d are defined by Eqs. (10)–(13), respectively.

For the fourth order approximation, the solution of Eq. (9) is given by

$$\varepsilon_e = E\left[-\frac{d}{4e} - \frac{1}{2}\sqrt{\frac{R}{3\sqrt[3]{2}e} - \frac{2c}{3e} + \frac{d^2}{4e^2} + \frac{\sqrt[3]{2}Q}{3eR}}\right.$$

$$\left. + \frac{1}{2}\sqrt{-\frac{R}{3\sqrt[3]{2}e} - \frac{4c}{3e} + \frac{d^2}{2e^2} - \frac{\sqrt[3]{2}Q}{3eR} - \frac{-d^3/e^3 + 4cd/e^2 - 8b/e}{4\sqrt{R/3\sqrt[3]{2}e - 2c/3e + d^2/4e^2 + \sqrt[3]{2}Q/3eR}}}\right]. \tag{A.3}$$

where

$$P = 2c^3 - 9bdc - 72aec + 27ad^2 + 27b^2e, \tag{A.4}$$

$$Q = c^2 - 3bd + 12ae, \tag{A.5}$$

$$R = \sqrt[3]{P + \sqrt{P^2 - 4Q^3}}, \tag{A.6}$$

where a, b, c, d, and e are defined by Eqs. (10)–(14), respectively. Using the above relations in conjunctions with Eqs. (4)–(6), relations for the third and the fourth order inversions and their associated errors are developed.

References

[1] A. Fatemi, L. Yang, Cumulative fatigue damage and life prediction theories: a survey of the state of the art for homogeneous materials, Int. J. Fatigue 20 (1) (1998) 9–34.
[2] H.A. Saab, D.A. Nethercot, Modeling steel frame behavior under fire conditions, Eng. Struct. 13 (4) (1991) 371–382.
[3] F.M. Mazzolani, V. Piluso, Prediction of the rotation capacity of aluminum alloy beams, Thin-Walled Struct. 27 (1) (1997) 103–116.
[4] J. Kaleta, G. Zietek, Representation of cyclic properties and hysteresis energy in alpha-brass using a certain class of elastic plastic models, Fatigue Fract. Eng. Mater. Struct. 17 (8) (1994) 919–930.
[5] S.C. Wong, Y.W. Mai, Effect of rubber functionality on mechanical and fracture properties of impact-modified nylon 6,6/polypropylene blends, Key Eng. Mater. 137 (1998) 55–62.
[6] T.K. Hight, J.F. Brandeau, Mathematical-modeling of the stress–strain strain rate behavior of bone using the Ramberg–Osgood equation, J. Biomech. 16 (6) (1983) 445–450.
[7] R.P. Skelton, H.J. Maier, H.J. Christ, The Baushinger effect, masing model and the Ramberg–Osgood relation for cyclic deformation in metals, Mater. Sci. Eng. A 238 (1997) 377–390.
[8] R. Bouc, Modele mathematique d'hysteresis (in French), Acustica 24 (1) (1967) 16–25.
[9] Y.K. Wen, Method for random vibration of hysteretic systems, J. Eng. Mech. ASCE 102 (2) (1976) 249–263.
[10] Y.K. Wen, Methods of random vibration for inelastic structures, Appl. Mech. Rev. 42 (2) (1989) 39–52.
[11] T.T. Baber, M.N. Noori, Random vibration of degrading, pinching systems, J. Eng. Mech. ASCE 111 (8) (1985) 1010–1026.
[12] M.N. Noori, J. Choi, H. Davoodi, Zero and nonzero mean random vibration analysis of a new general hysteresis model, Probabilistic Engineering Mechanic 1 (4) (1986) 192–201.
[13] G.C. Foliente, M.P. Singh, M.N. Noori, Equivalent linearization of generally pinching hysteretic, degrading systems, Earthquake Eng. Struct. Dyn. 25 (1996) 611–629.
[14] G. Ahmadi, F.C. Fan, M.N. Noori, A thermodynamically consistent model for hysteretic materials. Trans. B, Iran. J. Sci. Technol. Iran 21 (3) (1997) 257–278.
[15] N. Mostaghel, Analytical description of pinching, degrading hysteretic systems, J. Eng. Mech. ASCE 125 (2) (1999) 216–224.
[16] N. Mostaghel, R.A. Byrd, Analytical description of multidegree bilinear hysteretic systems, J. Eng. Mech. ASCE 126 (6) (2000) 588–598.
[17] M.V. Sivaselvan, A.M. Reinhorn, Hysteretic models for deteriorating inelastic structures, J. Eng. Mech. ASCE 126 (6) (2000) 633–640.
[18] I.D. Mayergoyz, Mathematical Models of Hysteresis, Springer, New York, Inc., NY, 1991.

[19] R.I. Stephens, A. Fatemi, R.R. Stephens, H.O. Fuchs, Metal Fatigue in Engineering, 2nd Edition, Wiley, New York, 2000.
[20] S. Wolfram, The Mathematica Book, 4th Edition, Wolfram Media/Cambridge University Press, Cambridge, 1999.
[21] N.E. Dowling, Mechanical Behavior of Materials, Engineering Methods for Deformation, Fracture, and Fatigue, 2nd Edition, Prentice-Hall, Englewood Cliffs, NJ, 1999.
[22] F. Ellyin, Fatigue Damage, Crack Growth and Life Prediction, Chapman & Hall, London, 1997.